THE JOURNAL OF BIOLOGICAL CHEMISTRY
Vol. 274, No. 49, Issue of December 3, pp. 35005–35011, 1999

Printed in U.S.A.

The Structures of the Horseradish Peroxidase C-Ferulic Acid Complex and the Ternary Complex with Cyanide Suggest How Peroxidases Oxidize Small Phenolic Substrates*

(Received for publication, May 27, 1999, and in revised form, August 23, 1999)

Anette Henriksen‡§, Andrew T. Smith¶, and Michael Gajhede‡

From the ‡Protein Structure Group, Department of Chemistry, University of Copenhagen, Universitetsparken 5, DK-2100 København Ø, Denmark and the ¶School of Biological Sciences, University of Sussex, Brighton BN1 9QG, United Kingdom

We have solved the x-ray structures of the binary horseradish peroxidase C-ferulic acid complex and the ternary horseradish peroxidase C-cyanide-ferulic acid complex to 2.0 and 1.45 Å, respectively. Ferulic acid is a naturally occurring phenolic compound found in the plant cell wall and is an *in vivo* substrate for plant peroxidases. The x-ray structures demonstrate the flexibility and dynamic character of the aromatic donor binding site in horseradish peroxidase and emphasize the role of the distal arginine (Arg^{38}) in both substrate oxidation and ligand binding. Arg^{38} hydrogen bonds to bound cyanide, thereby contributing to the stabilization of the horseradish peroxidase-cyanide complex and suggesting that the distal arginine will be able to contribute with a similar interaction during stabilization of a bound peroxy transition state and subsequent O-O bond cleavage. The catalytic arginine is additionally engaged in an extensive hydrogen bonding network, which also includes the catalytic distal histidine, a water molecule and Pro^{139}, a proline residue conserved within the plant peroxidase superfamily. Based on the observed hydrogen bonding network and previous spectroscopic and kinetic work, a general mechanism of peroxidase substrate oxidation is proposed.

Ferulic acid ((3-(4-hydroxy-3-methoxyphenyl)-2-propenoic acid, FA)[1] is a phenolic cinnamic acid derivative that is abundant in nature and known to act as an *in vivo* substrate for peroxidases (1). FA enhances the rigidity and strength of plant cell walls by cross-linking with pentosans, arabinoxylans, and hemicelluloses, thereby making the cell walls less susceptible to enzymatic hydrolysis during germination (2). The compound is a dibasic acid that exhibits an extended resonance stabilization of the phenolate anion, hence slightly increasing its acidity relative to phenol. pK_a values of 4.6 and 9.4 have been reported (3). Peroxidases have been reported to be the FA cross-linking catalyst (4). The level of FA and its derivatives seems to be positively correlated with protection of the plant against insects (5), fungal (6), viral (7), and avian (8) attack. In plants, FA is thought to arise from the conversion of cinnamic acid (9), and frequently it is esterified to hydroxyl groups of polysaccharides (10), flavonoids, and hydroxycarboxylic acids (11) and to plant sterols (12, 13).

The initial step in the biosynthesis of lignin is the enzymatic dehydrogenation of monolignols (14) to produce phenoxyl radicals. The radicals can link up to form dimers, trimers, and higher oligomers. Laccases and plant peroxidases have been proposed to be the *in vivo* generators of the phenoxyl radicals. The peroxidase oxidation of compounds with a syringyl group can be enhanced by esters of 4-coumaric acid and FA (15). For these reasons, it is of interest to study the interactions between the cell wall component FA and the well characterized horseradish peroxidase C.

Peroxidases catalyze the oxidative coupling of phenolic compounds using H_2O_2 as the oxidizing agent. The reaction is a three-step cyclic reaction by which the enzyme is first oxidized by H_2O_2 and then reduced in two sequential one-electron transfer steps from reducing substrates, typically a small molecule phenol derivative (the charges of heme propionates are ignored in the scheme).

$$\underset{\text{Native state}}{\text{HRPC}[(\text{Fe(III)})\text{Porph}^{2-}]^{+}} + H_2O_2 \rightarrow \underset{\text{Compound I}}{\text{HRPC}[(\text{Fe(IV)=O})\text{Porph}^{\cdot-}]^{\cdot+}} + H_2O$$

$$\text{HRPC}[(\text{Fe(IV)=O})\text{Porph}^{\cdot-}]^{\cdot+} + AH \rightarrow \underset{\text{Compound II}}{\text{HRPC}[(\text{Fe(IV)=O})\text{Porph}^{2-}]} + H^{+} + A^{\cdot}$$

$$\text{HRPC}[(\text{Fe(IV)=O})\text{Porph}^{2-}] + H^{+} + AH \rightarrow \text{HRPC}[(\text{Fe(III)})\text{Porph}^{2-}]^{+} + H_2O + A^{\cdot}$$

REACTIONS 1–3

The oxidized phenolic radicals polymerize with the final product depending on the chemical character of the radical, the environment, and the peroxidase isoenzyme used (4, 16). The oxidation of native enzyme by H_2O_2 (Reaction 1) is well understood, and numerous experiments (17) have confirmed the general catalytic mechanism for this step first proposed by Poulos and Kraut (18). The oxidation of phenolic substrates (Reactions 2 and 3) has been less well understood, but a histidine (19) (His^{42} in HRPC) and an arginine (20) (Arg^{38} in HRPC) have been shown to contribute significantly to enhance the rate of substrate oxidation.

The HRPC-CN-FA complex has a K_d for FA of 3.8 mM (21), which is 15-fold higher than the K_d of the HRPC-CN-benzhydroxamic acid (BHA). Like FA, most reducing substrates bind to peroxidases with dissociation constants in the mM range (22–24). There is, however, no direct correlation between the K_d of a substrate and its reactivity toward compounds I and II. In general the rates of reaction of compound I with substrates correlate well with the driving force for the reaction (25), the HOMO/LUMO energy levels of substrate molecules (26), or

* This work was supported by European Union Training and Mobility of Researchers program "Peroxidases in the Environment" Grant FMRX-CT98-0200 and by a grant from the Danish Natural Science Foundation (Danish syncrotron users). The costs of publication of this article were defrayed in part by the payment of page charges. This article must therefore be hereby marked "*advertisement*" in accordance with 18 U.S.C. Section 1734 solely to indicate this fact.

The atomic coordinates and structure factors (codes 6atj and 7atj) have been deposited in the Protein Data Bank, Brookhaven National Laboratory, Upton, NY.

§ To whom correspondence should be addressed: Protein Structure Group, Dept. of Chemistry, University of Copenhagen, Universitetsparken 5, DK-2100 København Ø, Denmark. Tel.: +45 35320273; E-mail:anette@jerne.ki.ku.dk.

[1] The abbreviations used are: FA, ferulic acid; BHA, benzhydroxamic acid; CN, cyanide; HRPC, horseradish peroxidase C.

their calculated ionization potentials (27). FA acid is, however, an excellent substrate for HRPC (see later), the immediate product being diferulic acid (4).

The formation of stable complexes between a variety of aromatic donor molecules including FA and the CN adduct of HRPC has been studied extensively by NMR techniques (21). The CN bound state of the enzyme has been preferred by NMR spectroscopists because of its low spin nature. In crystallographic studies, the oxyperoxidase complex (Compound III) has served as a model for the Fe^{3+}-OOH^- species, a labile intermediate in the formation of Compound I (28, 29).

In this crystallographic study, we describe the structure of the HRPC-CN-FA complex, which serves as a model for the pre-electron transfer complex formed between FA and compounds I and II. The presence of cyanide at the sixth coordination position of the heme iron sterically hinders the distal heme pocket and to some extent parallels the effect of the ferryl oxygen in Compounds I and II. Based on the structures of the HRPC-FA and HRPC-CN-FA complexes, we propose a general mechanism for oxidation of small phenolic substrates.

EXPERIMENTAL PROCEDURES

Presteady State Kinetic Measurements—The second order rate constants for the reduction of compounds I and II were determined as described previously (30) under pseudo-first order conditions. Plots of k_{obs} *versus* substrate concentration were linear over the range studied, which were: 2.5–15 μM for ferulic acid, 1–9 mM for indole-3-propionic acid, 1–8 mM for *p*-aminobenzoic acid, and 15–75 μM for ferrocyanide. All measurements were conducted at 25 ± 0.2 °C in 10 mM sodium phosphate buffer, pH 7.0, on an Applied Photo Physics SX18MV stopped flow system.

Crystallization—Crystals were grown from a mixture of equal amounts (2 μl) of recombinant HRPC and reservoir solution and 1 μl of saturated FA in 2-propanol by hanging drop vapor diffusion at 10 °C. The drops were equilibrated against a reservoir of 20% (w/v) polyethylene glycol 8000, 0.2 M $Ca(CH_3COO)_2$, and 0.1 M cacodylate buffer at pH 6.5. Immediately prior to data collection the crystals were immersed to a cryo-protective solution consisting of 30% (w/v) polyethylene glycol 8000, 0.2 M $Ca(CH_3COO)_2$, and 0.1 M cacodylate buffer, pH 6.5. At 120 K the crystals were orthorhombic, space group $P2_12_12_1$, with unit cell dimensions a = 40.3 Å, b = 67.3 Å, and c = 117.6 Å. A ternary complex of HRPC, cyanide, and ferulic acid was prepared by adding 1 μl of 10 mM KCN to the equilibrated drops. The crystals were allowed to soak with KCN for 4 h. The space group of this complex was $P2_12_12_1$, and the unit cell dimensions were a = 40.9 Å, b = 66.9 Å, and c = 119.0 Å at 100 K.

Data Collection and Reduction—Diffraction data for the HRPC-FA were collected at 120 K on a Rigaku R-axis IIC image plate system with a Rigaku RU200 rotating anode operated at 180 mA and 50 kV. The crystal to detector distance was 80 mm, and 90 successive frames of 1° oscillations were collected. The frame exposure time was 30 min. The HRPC-CN-FA diffraction data were collected at MAXLABII, University of Lund at beamline 711 at 100 K. A MAR345 image plate system was used for this data collection, which had a crystal to detector distance of 200 mm and an oscillation range of 0.75°. The 345-mm/150-μm scanner of the MAR345 was utilized. Auto-indexing and integration of intensities was achieved with Denzo (31), whereas the data were averaged and scaled with Scalepack (31). Statistics for the data processing are given in Table I. Data were collected to a minimum Bragg spacing of 2.0 Å for the HRPC-FA complex, whereas the HRPC-CN-FA data were collected to a minimum Bragg spacing of 1.47 Å.

Structure Determination and Refinement—The structures were solved by molecular replacement (32) using the structure of native HRPC (Protein Data Bank code 1atj) as the search model including only the protein moiety. Iterative rounds of model building in O (33) were followed by refinement in CNS (34) for the HRPC-FA structure and in SHELX-97 (35) for the HRPC-CN-FA structure. The occupancies of the FA molecules were refined within the limit 0–1 for the HRPC-FA complex but without restraining the sum of occupancies. The final occupancies of FA1, FA2, and FA3 were 0.36, 0.46, and 0.26, respectively. The only heme group restraints applied in the SHELX refinement was the restraining of chemically equivalent bonds to have equal bond length (SADI) (Table II). The FA molecules bonds and angles were restrained to values obtained from the small molecule data base, Cambridge Structural Database, and the Engh and Huber parameters (36) were used to restrain the protein geometry in both complexes. Iron, calcium, and sulfur atoms were refined anisotropically in the SHELX-97 refinements. The SHELX refinement consisted of four rounds of conjugate gradient least square refinement and was completed by a blocked full-matrix refinement. Refinement statistics are listed in Table I. In addition to the FA molecule found in the active site of the HRPC-CN-FA complex, another well defined FA molecule is found in the HRPC-CN-FA crystal. In the HRPC-FA crystals, a poorly defined and not accounted for $2\sigma F_o - F_c$ electron density is observed in the same location. This FA molecule is positioned between symmetry related HRPC molecules, having <4.5 Å to the N-terminal (residues Asn^{13}, Asn^{16}, Ile^{17}, and Asp^{20} in helix A) of one HRPC molecule and <4.5 Å to part of the loop forming the proximal Ca^{2+} site (residues Leu^{223}, Arg^{224}, Thr^{225}, and Lys^{232}) of a second HRPC molecule. Except Thr^{225}, which is a proximal calcium ligand in class II and class III plant peroxidases, none of these contact residues are conserved among the plant peroxidase superfamily, and only crystal packing relevance and no enzymatic significance is ascribed to this interaction. Refinements include residues 1–305 of the HRPC-CN-FA complex and residues 1–306 of the HRPC-FA complex. An N-terminal methionine (Met^0 originating from the recombinant expression (37)) had only faint electron density in both cases and was omitted from the refinement. The C-terminal serine and aspargine were omitted in the case of the HRPC-CN-FA complex, whereas the C-terminal aspargine was omitted from the refinement of the HRPC-FA complex because of missing or weak electron density. The residues Asn^{16}, Ser^{89}, Cys^{91}, Arg^{178}, Ser^{188}, Thr^{200}, Val^{219}, Lys^{232}, Gln^{240}, Glu^{249}, Ser^{265}, Asn^{286}, and Val^{304} of the HRPC-FA complex were refined in two alternate conformations, the relative occupancy of the two conformations were no refined but fixed at 0.5. In the HRPC-CN-FA complex residues Ser^{10}, Asn^{16}, Asn^{24}, Arg^{27},

TABLE I
Statistics for crystallographic structure determination

	HRPC-FA	HRPC-CN-FA
Data collection		
Wavelength (Å)	1.54	1.015
Resolution range (Å)	29–2.0	34–1.47
Observations	108409	379088
Unique reflections	21778	51544
Completeness (%)[a]	97.2 (96.0)	91.2 (82.7)
R_{sym} (%)[a,b]	7.6 (20.8)	7.2 (25.8)
Refinement		
Resolution range (Å)	29–2.0	34–1.47
Unique reflections ($I > 0$)	21751	51442
R_{cryst} (%)[c]	0.166	0.160
R_{free} (%)[d]	0.199	0.203
Number of nonhydrogen atoms		
Protein	2469	2430
Solvent	399	440
Heterogen atoms	87	75
Root mean square deviations from ideal values		
Bond length (Å)	0.01[e]	0.01[f]
Bond angle (°)	1.4[e]	
Angle distances (Å)		0.026[f]
Estimated coordinate error (Å)		
Luzzati plot	0.18[e]	0.16[f]
Ramachandran plot[g]		
Residues in most favored (disallowed) regions (%)	88.1 (0.0)	90.0 (0.0)
Mean B-factor (Å^2)		
Protein	9.8	11.7
Heme	6.8	7.4
Ferulic acid	18.5	27.2
Solvent	22.9	29.1

[a] Numbers in parenthesis are for the highest resolution shell, 2.07–2.00 Å for HRPC-FA and 1.50–1.47 Å for HRPC-CN-FA.

[b] $R_{sym} = \Sigma_{hkl}(\Sigma_i(|I_{hkl,i} - \langle I_{hkl}\rangle|))/\Sigma_{hkl,i}\langle I_{hkl}\rangle$, where $I_{hkl,i}$ is the intensity of an individual measurement of the reflection with Miller indicies h, k, and l and $\langle I_{hkl}\rangle$ is the mean intensity of that reflection.

[c] $R_{cryst} = \Sigma_{hkl}(||F_{o,hkl}| - |F_{c,hkl}||)/|F_{o,hkl}|$, where $|F_{o,hkl}|$ and $|F_{c,hkl}|$ are the observed and calculated structure factor amplitudes.

[d] R_{free} is equivalent to the R-factor but calculated with reflections omitted from the refinement process (5% of reflections omitted).

[e] Calculated with the program CNS (34).

[f] Calculated with the program SHELX-97 (35).

[g] Calculated with the program PROCHECK (62).

TABLE II
Geometry of the cyanide bound heme
The distances and angles are followed by standard deviation in parentheses.

Distances		Angles		Dihedrals	
	Å		*degrees*		*degrees*
Fe-C (CN)	1.99 (3)	Fe-C-N	159 (3)	pyrrole N plane to pyrrole I	5 (1)
H42 N_E-N (CN)	2.67 (4)	pyrrole N_I-Fe-C	83 (1)	pyrrole N plane to pyrrole II	6 (1)
H170 N_E-Fe	2.08 (3)	pyrrole N_{II}-Fe-C	82 (1)	pyrrole N plane to pyrrole III	9 (1)
Fe-pyrrole N plane	0.073 (5)	pyrrole N_{III}-Fe-C	90 (1)	pyrrole N plane to pyrrole IV	7 (1)
C(CN)-N(CN)	1.14 (5)	pyrrole N_{IV}-Fe-C	96 (1)		
		C-N-N_E (His^{42})	145 (3)		

Ile^{80}, Cys^{91}, Gln^{147}, Ser^{151}, Asn^{158}, Ser^{161}, Lys^{174}, Arg^{178}, Asp^{182}, Thr^{200}, Arg^{264}, Ser^{265}, and Ile^{297} were refined with alternate conformations. In this case, the relative occupancies were refined, but the sum of the occupancies was restricted to 1.0.

RESULTS AND DISCUSSION

Reactivity of Ferulic Acid toward HRPC Compounds I and II

Table III shows the measured second order rate constants for the oxidation of FA by HRPC compounds I and II. FA is notable because its reaction with compound II is remarkably fast, in comparison with the other substrates listed in Table III and up to 10 times faster than many other phenols. It is a candidate for one of the most reactive physiological substrates oxidized by HRPC. This suggests that the structure of any pre-electron transfer complex between compound II and FA is close to optimal.

TABLE III
Second order rate constants for the reduction of HRPC compounds I and II by ferulic acid and comparison with other substrates
All second order rate constants were determined with recombinant HRPC (63) under pseudo-first order conditions at pH 7.0 in 10 mM sodium phosphate as described under "Experimental Procedures."

Substrates for HRPC compounds I and II	Bimolecular rate constants for compound I reduction (k_2)	Bimolecular rate constants for compound II reduction (k_3)
	$M^{-1}\ s^{-1}$	$M^{-1}\ s^{-1}$
Ferulic acid	$4.8 \pm 0.2 \times 10^7$	$1.3 \pm 0.01 \times 10^7$
Indole-3-propionic acid	$6.6 \pm 0.1 \times 10^3$	$4.0 \pm 0.1 \times 10^2$
p-Aminobenzoic acid	$6.5 \pm 0.3 \times 10^3$	$4.9 \pm 0.1 \times 10^2$
Ferrocyanide	$1.4 \pm 0.05 \times 10^7$	$2.1 \pm 0.1 \times 10^5$

X-ray Structure

Overall Structure of the HRPC-FA Complexes—The crystals used in this study represent a new crystal form compared with the structure of HRPC (38) and of the HRPC-BHA complex (37). The overall structure of HRPC is the same in all four structures with an overall root mean square deviation for C_α positions <0.4 Å in a pairwise superposition of the structures. The most significant side chain rearrangements close to the active site are found for residues Phe^{68}, Asn^{135}, Phe^{142}, Phe^{143}. and Phe^{179}. The repositioning of Phe^{68} in the crystal structure of the HRPC-BHA complex effectively "closes the lid" on the substrate access channel optimizing the substrate-protein interactions for this unusual but nonphysiological tight binding substrate (37) (K_d 2.5 μM). Phe^{68} also contacts Asn^{135}, which shows a significant adjustment when Phe^{68} alters conformation. In the HRPC-FA and the HRPC-CN-FA complexes, Phe^{68} is in an "open lid" orientation, but the residue is repositioned 1.6 Å relative to its position in the native HRPC structure (38). A 0.8 Å reposition of Asn^{135} is a consequence of the Phe^{68} reposition. In more general terms, it seems that the binding of substrate in the substrate access channel cause approaching of distal side residues toward the substrate ($Phe^{68} > Asn^{135} > Asp^{132} > Leu^{131}$). The effect is more pronounced for BHA than for FA. Also side chain movements of 0.8 Å (Phe^{179}), 0.7 Å (Phe^{142}), and 0.4 Å (Phe^{143}) are observed when comparing the structures of the HRPC-FA complexes with the structure of native HRPC. However, a closer spatial proximity of Ala^{140} and Phe^{142}, Phe^{143} as observed by NMR when the HRPC-CN-BHA and the HRPC-CN complexes was compared (39) cannot be observed when comparing the x-ray structures of the HRPC-CN-FA complex and the native state of HRPC. The flexibility of the aromatic binding pocket of HRPC to accommodate small molecule substrates seems to be a characteristic feature of this site.

FA Binding Sites in the HRPC-FA Complex—The 2 $F_o - F_c$ simulated anneal omit (the FA molecules and residues within a 3.5 Å radius were omitted) difference electron density map in the active site of the HRPC-FA complex is shown in (Fig. 1*A*). The relative weaknesses of the substrate density and its extent suggest both partial occupancy and multiple binding sites or substrate orientations. The disorder in the electron density of the substrate does not allow us to model the orientation of FA unambiguously, but conclusions about substrate orientation can be drawn. The disordered density can be described by at least three FA binding modes (Fig. 1). The positions of the three possible binding modes are too close to represent more than one FA molecule bound in or close to the active site simultaneously (Fig. 1*A*). 3σ $F_o - F_c$ electron densities was observed over the heme iron at the position of the FA carboxylic oxygens of FA3 (Fig. 1*D*), when the occupancies of the three FA models were refined. This excess electron density could be accounted for by modeling two partly occupied water molecules in these positions (Fig. 1, *B* and *C*). The FA3 binding mode (Fig. 1*D*) (carboxylate facing inwards) is a direct consequence of the use of unesterified FA. *In vivo*, FA would be esterified to the hydroxyl groups of polysaccharides preventing the FA3 orientation from occurring. The ferryl oxygen of compounds I and II would sterically be in conflict with the FA3 binding mode, leading to the prediction that high FA concentrations *in vitro* might lead to substrate inhibition, by competitively slowing the reaction of the enzyme with hydrogen peroxide. This has been reported for certain substrates (40), but we are not aware of any detailed kinetic analyses of FA oxidation by HRPC. The FA1 and FA2 binding modes (Fig. 1, *B* and *C*) are the likely modes for productive interaction with compounds I and II *in vivo*. The positive $F_o - F_c$ difference electron density observed suggest that at least two water molecules are bound in the active site when the substrate binds in the FA1 or FA2 orientations. One of these water molecules is the molecule found between the heme iron and the distal histidine residue in the resting state structures of plant peroxidases (38, 41–46). The second water molecule in the active site of the HRPC-FA complex hydrogen bonds to Pro^{139}. This residue and associated water are conserved in the <2.0 Å resolution structures of other plant peroxidases including *Arthromyces ramosus* peroxidase (47) (1.9 Å), lignin peroxidase (48) (1.7 Å), and barley peroxidase (46) (1.9 Å), all of

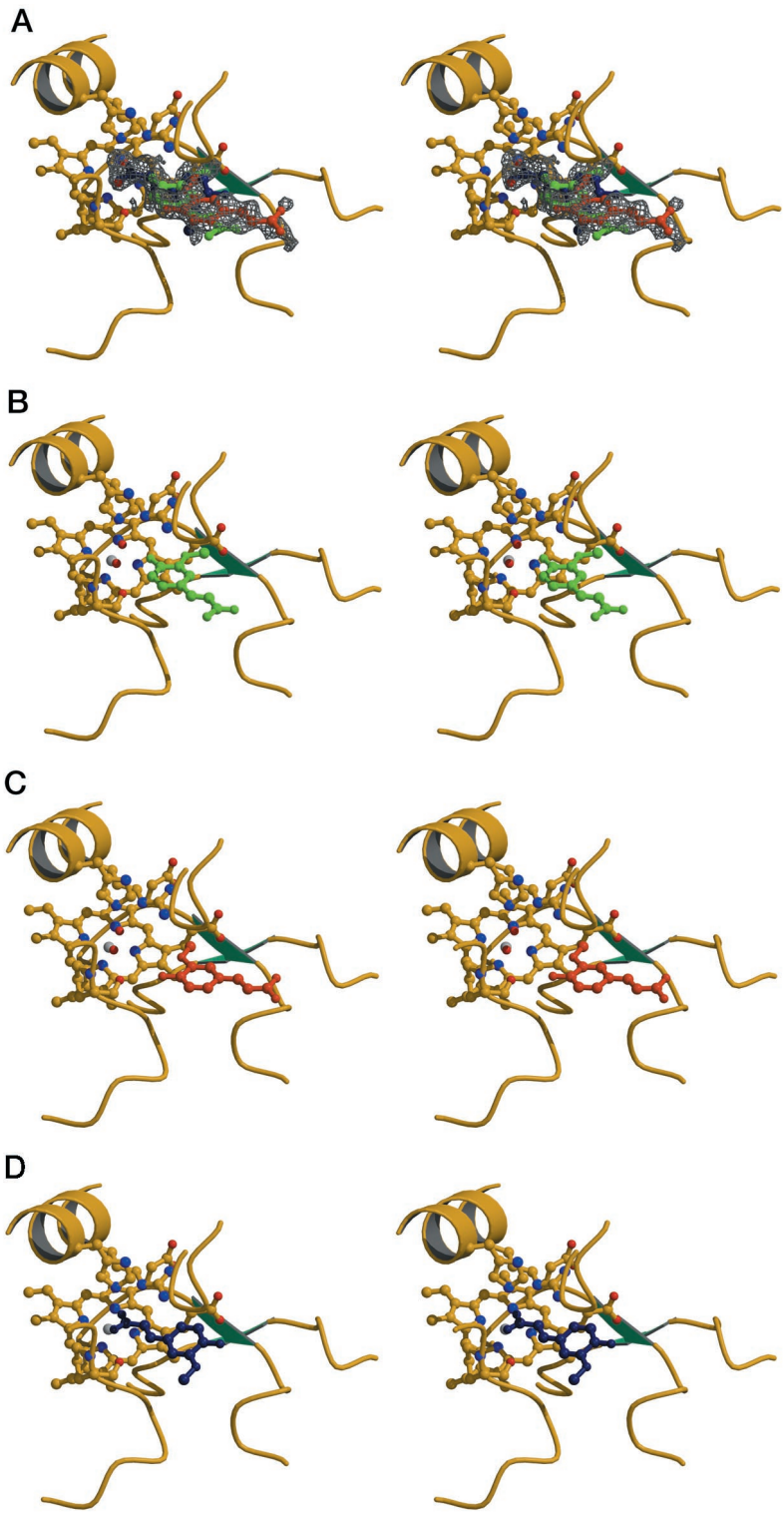

FIG. 1. *A*, the active site of the HRPC-FA complex showing the three possible binding modes, FA1, FA2, and FA3, of FA (59–61). The 0.5σ 2 $F_o - F_c$ simulated anneal omit electron density surrounding the FA molecules is included. The occupancies of the FA molecules were refined to 0.36, 0.46, and 0.26 for the FA1, the FA2, and the FA3, respectively. *B*, the active site of the HRPC-FA complex with FA1 bound. *C*, the active site of the HRPC-FA complex with FA2 bound. *D*, the active site of the HRPC-FA complex with FA3 bound. In *C* and *D* two partly occupied water molecules are included in the active site modeled on the basis of excess $F_o - F_c$ electron density at these positions.

which in the active state oxidize small aromatic substrates rapidly.

The products typically resulting from the oxidation of substrates are phenoxyl radicals, very similar in structure to their respective substrate molecule but chemically very reactive species. These leave the active site rapidly and polymerize or disproportionate. A prolonged retention of the radical in close proximity to the heme group could increase the risk of autooxidative damage; therefore loose association of the reducing substrate with the enzyme, as found in the x-ray structure of the HRPC-FA complex, could be an advantage. It may be for this reason that the production of the very reactive veratryl alcohol cation radical in lignin peroxidase is displaced to a surface tryptophan residue (49) some distance from the heme.

FA Binding Site in the HRPC-CN-FA Complex—The 2 $F_o - F_c$ simulated omit (omitting FA, CN, and residues within a radius of 3.5 Å) electron density in the active site of the HRPC-CN-FA complex is shown in Fig. 2*A*. This electron density can be unambiguously modeled by a cyanide molecule ligated to the sixth coordination position of the heme iron and by a single unique FA binding mode in the active site, as shown in Fig. 2*B*. The phenolic oxygen of FA is hydrogen bonded to Arg^{38} N_{H2}

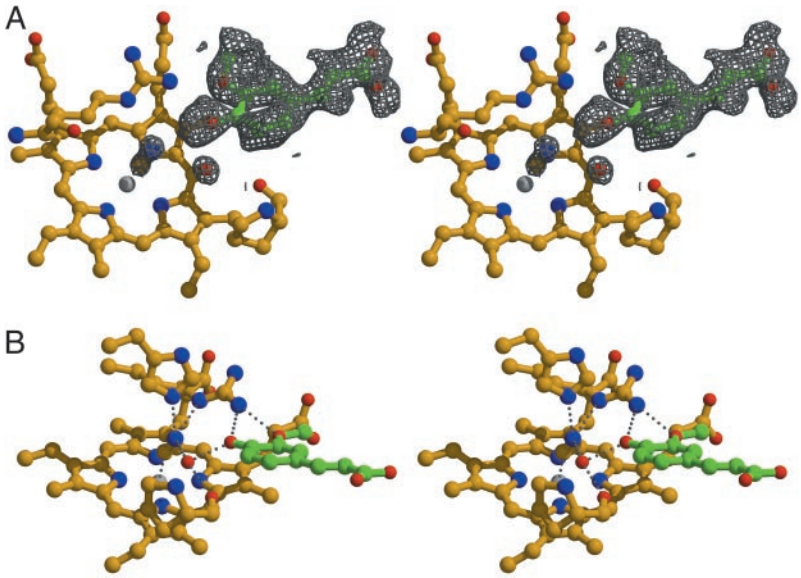

FIG. 2. *A*, the 1.5σ simulated anneal omit 2 $F_o - F_c$ density surrounding the cyanide and the water molecule in the active site of the HRPC-CN-FA complex and the 0.3σ simulated anneal omit 2 $F_o - F_c$ density surrounding FA molecules in the HRPC-CN-FA complex. *B*, the active site of HRPC-CN-FA. Hydrogen bonds between active site residues and ligands are indicated with *dotted black lines*.

(3.0 Å) and the methoxy oxygen of FA is hydrogen bonded to the same arginine nitrogen (3.2 Å). A short hydrogen bond distance is found between the phenolic oxygen and an active site water molecule (2.6 Å) (Fig. 2*B*). This water molecule is hydrogen bonded both to the backbone oxygen of Pro^{139} (2.9 Å) and to the cyanide nitrogen (2.9 Å). The rest of the interactions between the FA molecule and HRPC can be defined as hydrophobic. HRPC residues within a 4.0 Å contact distance of FA are Phe^{68}, Gly^{69}, Pro^{139}, Ala^{140}, Phe^{142}, Phe^{179}, and the C-18 methyl and C-20 of the heme group. The shortest distance between the heme group and the FA molecule is found between the methoxy oxygen and the heme C-18 methyl (3.5 Å). The distance between the phenolic oxygen and heme C-20 distance is 3.9 Å. The active site water molecule is 3.5 Å from His^{42} and an almost equal distance (3.6 Å) from the cyanide carbon. The aromatic ring of FA is almost coplanar with the heme, and the general electron transfer is likely to take place from the highest occupied π-orbital of the FA to the heme π-orbital.

It could be argued that the position of the FA molecule in the HRPC-CN-FA complex is affected by the presence of the diatomic cyanide ion in the active site and that a ferryl oxygen ligand could result in a different orientation of the FA molecule. However, the position of the FA molecule in the HRPC-CN-FA complex corresponds to the position of FA1 in the active site of the HRPC-FA complex (Fig. 1*B*). A superposition of the HRPC-CN-FA complex and the HRPC-BHA complex shows additionally that the position of the aromatic rings in these two complexes coincide. In both the HRPC-FA and the HRPC-BHA complexes, a water molecule is positioned between the heme iron and the distal histidine. This suggests that although the sixth coordination position in compound I or II is occupied by a single atom, the orientation of the FA molecule in the HRPC-CN-FA complex is likely to be the same as it would be in a complex with compound I or II.

The change in number of FA binding modes seen between the HRPC-FA and the HRPC-CN-FA complex is obviously caused directly by the presence of CN, because His^{42} is the only residue that significantly changes position when cyanide is bound to the HRPC-FA complex. The presence of cyanide in the active site effectively excludes the FA3 binding mode. The FA2 binding mode provides only one direct hydrogen bond between substrate and protein, whereas the FA1 binding mode provides two direct hydrogen bonds. Because the cyanide can serve as a hydrogen bond acceptor for the active site water molecule to which FA1 binds (Fig. 2*B*), it must be expected that the through water hydrogen bonds in the active site of the HRPC-CN-FA complex additionally will favor the FA1 binding mode. In contrast, the water molecule directly above heme iron in the HRPC-FA1 complex (Fig. 1*B*) will serve as a hydrogen bond donor to the active site water molecule. This makes the active site water molecule a hydrogen bond donor to the phenolic oxygen and weakens the FA1 binding in the HRPC-FA complex. Like cyanide, a ferryl oxygen will act as a hydrogen bond acceptor in the active site of HRPC.

At least two structural features are likely to explain the rapid reduction rates of compounds I and II by FA: (i) The structure of FA, with a methoxy group in the ortho position of the phenol, aids positioning this substrate in the substrate access channel. The result is hydrogen bonds from the substrate to both Arg^{38} and the active site water molecule, which are close to optimal. (ii) FA has an extended resonance stabilization of the phenolate anion but is still fitting perfectly into the substrate access channel.

The Orientation of the Cyanide Molecule in the Active Site—The 1.47 Å resolution of the HRPC-CN-FA data allowed us to perform an unrestrained refinement of the positions of the FA and the CN species. The shape of the cyanide electron density distinctly approaches atomicity with respect to the carbon and the nitrogen atoms of the cyanide ion (Fig. 2*A*). Prior to compound I formation (reaction 1), a transient Fe^{3+}-OOH^- intermediate is likely to be formed, where the peroxide proton has been transferred to the distal histidine (18, 50). To further characterize the mechanism behind heterolytic O-O bond cleavage, it has been of interest to structurally characterize this intermediate. Because of the fast nature of subsequent O-O bond cleavage, it has been difficult to demonstrate the existence of such an intermediate, even in solution (51). The formation of a diatomic ligand complex such as the HRPC-CN complex could to some extent mimic the transient intermediate despite the chemical differences between the O-OH^- and the C≡N^- species. Superimposing the structures of native HRPC, the HRPC-BHA complex, the HRPC-FA complex, and the HRPC-CN-FA complex show that the position of the active site histidine is affected by the binding of CN^-. His^{42} N_{E2} moves 0.5 Å toward the cyanide nitrogen, hereby supplying a short hydrogen bond (2.7 Å) to stabilize the binding of the ligand (Fig. 2*B*). Surprisingly, the side chain of the distal arginine does not move when CN^-, BHA, or FA is bound to HRPC, yet Arg^{38} N_E stabilizes CN^- binding with a hydrogen bond (2.9 Å) to the cyanide nitrogen. Therefore we suggest that Arg^{38} could be

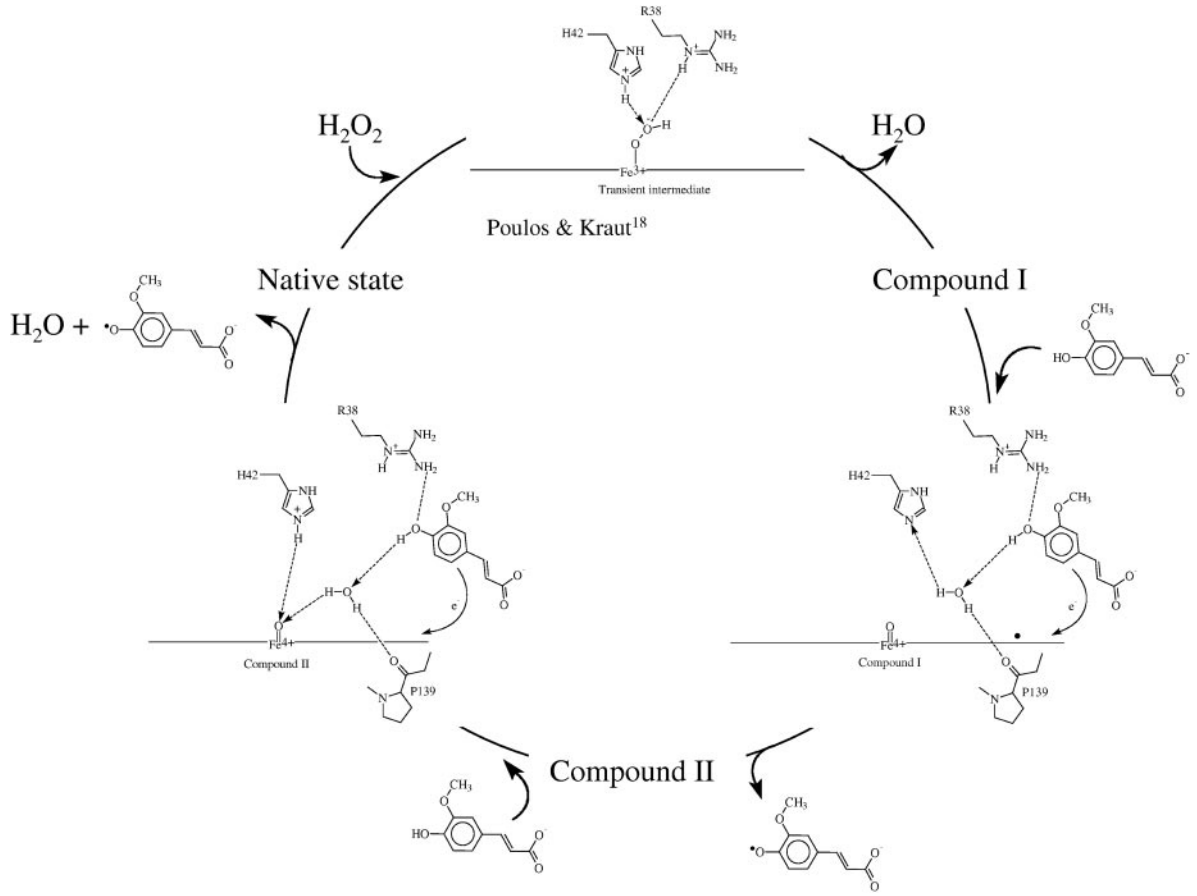

FIG. 3. **Proposed mechanism for substrate oxidation in plant peroxidases.** First, the active site arginine (Arg^{38} in HRPC) donates a hydrogen bond to the phenolic oxygen of the reducing substrate. This hydrogen bond will assist proton transfer from the phenolic oxygen to active site histidine (His^{42} in HRPC) through an active site water molecule held in position by the backbone oxygen of a conserved proline residue (Pro^{139} in HRPC). The electron is transferred to the heme group via the C-18 methyl-C-20 heme edge. Then compound II reduction is assisted by similar a proton transfer. The proton can be transferred to the ferryl oxygen through the active site water molecule situated equidistant between the distal histidine and the expected position of the ferryl oxygen of compound II, regenerating the resting state enzyme and a water molecule.

assisting heterolytic O-O bond cleavage by acting as a hydrogen bond donor to the transient Fe^{3+}-OOH^- intermediate, in contrast to the situation proposed in cytochrome *c* peroxidase (28). This suggestion is supported by the fact that the active site Arg → Lys mutant of HRPC showed a 500-fold decrease in the rate of compound I formation (52), whereas the similar cytochrome *c* peroxidase mutation showed only a 2-fold decrease in rate (53). In cytochrome *c* peroxidase, a tryptophan in the active site can also assist in the heterolytic O-O bond cleavage.

Mechanism for Substrate Oxidation in Plant Peroxidases—As argued previously, the orientation of FA is likely to be close to identical in the HRPC-CN-FA complex and in compound I and II complexes with FA. The position of the distal site arginine is invariant in the HRPC, HRPC-BHA, HRPC-FA, and the HRPC-CN-FA structures. This additionally suggests that the position of Arg^{38} is insensitive to the ligand composition of the active site and that the position of Arg^{38} is likely to be the same also in compounds I and II.

As noted, the water molecule found in the active site of the HRPC-FA and HRPC-CN-FA complexes (Fig. 2) is also observed in the active sites of other high resolution structures of plant peroxidases. The proline residue supplying the backbone oxygen that is the hydrogen bond acceptor for the water molecule is conserved throughout the plant peroxidase superfamily. If we assume the cyanide carbon atom to be in approximately the same position as the ferryl oxygen in compounds I and II, it is evident that the active site water molecule will be able to play a very significant role in the oxidation of substrate molecules. Arg^{38} N_E is then found to be within hydrogen bonding distance of the expected position of the ferryl oxygen of compounds I and II (3.4 Å from N_E to the cyanide carbon) and will be able to stabilize these states with a hydrogen bond similar to what is seen in cytochrome *c* peroxidase compound I (54) and as suggested by the cytochrome *c* peroxidase-fluoride complex (29, 55). However, as FA binding to HRPC includes a hydrogen bond between the phenolic oxygen and Arg^{38} N_{H2} (2.9 Å), the hydrogen bond to ferryl oxygen will be weakened by substrate binding. The center of gravity of the charge distribution of Arg^{38} will be moving from N_E toward N_{H2}, and substrate binding is likely to be an activator of the ferryl center of compounds I and II of HRPC.

The oxidation of substrate molecules by plant peroxidases is accompanied by proton transfer (reactions 2 and 3 and Fig. 3). The hydrogen bond between Arg^{38} N_{H2} and phenolic oxygen will assist proton transfer from the phenol to the distal histidine or ferryl oxygen as outlined in Fig. 3. Site-directed mutagenesis studies support the notion that Arg^{38} can interact with the reducing substrate (56). The final destination of the proton is the distal histidine in the case of compound I reduction (57). An electron is transferred from the phenolate to the C-18 methyl-C-20 edge of the heme group (58), and the resulting radical will dissociate from the enzyme. In the case of compound II reduction, the distal arginine assists the proton transfer with an equivalent hydrogen bond to the phenolic oxygen of a second substrate molecule. Here the final destination of the proton is the ferryl oxygen, and an electron is

transferred to the heme. Both proton transfers can well involve the water molecule, which is positioned equidistant between the active site histidine and the anticipated position of the ferryl oxygen in compounds I and II.

Conclusions

The aromatic donor binding region in plant peroxidases is a flexible solvent exposed region that allows for fast exchange of solvent molecules and small phenolic compounds. It cannot be considered a substrate binding site in the classical sense. The orientation of the FA molecule in the HRPC-FA-CN complex reveals the possible general enzymatic mechanism for plant peroxidase substrate oxidation: the distal arginine will assist proton transfer by hydrogen bonding to the phenolic oxygen. A structurally conserved water molecule positioned equidistant between the active site histidine and the expected position of the ferryl oxygen provides the highway for proton transfer. The final destination of the proton is the distal histidine in the case of compound I reduction and the ferryl oxygen in the case of compound II reduction.

REFERENCES

1. Fry, S. C. (1986) in *Molecular and Physiological Aspects of Plant Peroxidases* (Greppin, H., Penel, C., and Gaspar, T., eds) pp. 169–182, University of Geneva, Geneva
2. Fulcher, R. G., O'Brien, T. P., and Lee, J. W. (1972) *Aust. J. Biol. Sci.* **25,** 23–34
3. Kenttämaa, J., Räisänen, S., Auterinen, L., and Lindberg, J. J. (1970) *Suom. Kemistilehti B.* **43,** 333–336
4. Markwalder, H. U., and Neukom, H. (1976) *Phytochemistry* **15,** 836–837
5. Suga, T., Ohta, S., Munesada, K., Ide, N., Kurokawa, M., Shimizu, M., and Ohta, E. (1993) *Phytochemistry* **33,** 1395–1401
6. Putman, L. J., Laks, P. E., and Pruner, M. S. (1989) *Holzforschung* **43,** 219–224
7. Martin-Tanguy, J. (1985) *Plant Growth Regul.* **3,** 381–399
8. Greig-Smith, P. W., and Wilson, M. F. (1989) U.K. patent 88-29167
9. Gross, G. G. (1985) in *Biosynthesis and Biodegradation of Wood Components* (Higuchi, T., ed) pp. 229–271, Academic Press, Inc., Orlando
10. Meyer, K., Kohler, A., and Kauss, H. (1991) *FEBS Lett.* **290,** 209–212
11. Herrmann, K. (1989) *CRC Crit. Rev. Food. Sci. Nutr.* **28,** 315–347
12. Seitz, L. M. (1989) *J. Agric. Food. Chem.* **37,** 662–667
13. Evershed, R. P., Spooner, N., Prescott, M. C., and Goad, L. J. (1988) *J. Chromatogr.* **440,** 23–35
14. Freudenberg, K. (1965) *Science* **148,** 595–600
15. Takahama, U., and Oniki, T. (1996) in *Plant Peroxidases: Biochemistry and Physiology* (Obinger, C., Burner, U., Ebermann, R., Penel, C., and Greppin, H., eds) pp. 118–123, University of Geneva, Geneva
16. Frías, I., Siverio, J. M., González, C., Trujillo, J. M., and Pérez, J. A. (1991) *Biochem. J.* **273,** 109–113
17. Erman, J. E., Vitello, L. B., Miller, M. A., and Kraut, J. (1992) *J. Am. Chem. Soc.* **114,** 6592–6593
18. Poulos, T. L., and Kraut, J. (1980) *J. Biol. Chem.* **255,** 8199–8205
19. Rodriguez-Lopez, J. N., Smith, A. T., and Thorneley, R. N. F. (1996) *J. Bioinorg. Chem.* **1,** 136–142
20. Rodriguez-Lopez, J. N., Smith, A. T., and Thorneley, R. N. F. (1996) *J. Biol. Chem.* **271,** 4023–4030
21. Veitch, N. C. (1995) *Biochem. Soc. Trans.* **23,** 232–240
22. Leigh, J. S., Maltempo, M. M., Ohlsson, P. I., and Paul, K. G. (1975) *FEBS Lett.* **51,** 304–308
23. Morishima, I., and Ogawa, S. (1979) *J. Biol. Chem.* **254,** 2814–2820
24. Paul, K. G., and Ohlsson, P. I. (1978) *Acta Chem. Scand.* **B 32,** 395–404
25. Candeias, L. P., Folkes, L. K., Porssa, M., Parrick, J., and Wardman, P. (1996) *Biochemistry* **35,** 102–108
26. Sakurada, J., Sekiguchi, R., Sato, K., and Hosoya, T. (1990) *Biochemistry* **29,** 4093–4098
27. Rietjens, I. M. C. M., Osman, A. M., Veeger, C., Zakharieva, O., Antony, J., Grodzicki, M., and Trautwein, A. X. (1996) *J. Biol. Inorg. Chem.* **1,** 372–376
28. Miller, M. A., Shaw, A., and Kraut, J. (1994) *Nat. Struct. Biol.* **1,** 524–531
29. Edwards, S. L., and Poulos, T. L. (1990) *J. Biol. Chem.* **265,** 2588–2595
30. Smith, A. T., Sanders, S. A., Thorneley, R.-N. F., Burke, J. F., and Bray, R.-R. C. (1992) *Eur. J. Biochem.* **207,** 507–519
31. Otwinowski, Z., and Minor, W. (1997) *Methods Enzymol.* **276,** 307–326
32. Navaza, J. (1994) *Acta Crystallogr.* **A50,** 157–163
33. Jones, A., Zou, J. Y., Cowan, S. W., and Kjeldgaard, M. (1991) *Acta Crystallogr.* **A47,** 110–119
34. Brünger, A. T., Adams, P. D., Clore, G. M., DeLano, W. L., Gros, P., Grosse-Kunstleve, R. W., Jiang, J.-S., Kuszewski, J., Nilges, M., Pannu, N. S., Read, R. J., Rice, L. M., Simonson, T., and Warren, G. L. (1998) *Acta Crystallogr.* **D54,** 905–921
35. Sheldrick, G. M., and Schneider, T. R. (1997) *Methods Enzymol.* **277B,** 319–343
36. Engh, R. A., and Huber, R. (1991) *Acta Crystallogr.* **A47,** 392–400
37. Henriksen, A., Schuller, D. J., Meno, K., Welinder, K. G., Smith, A. T., and Gajhede, M. (1998) *Biochemistry* **37,** 8054–8060
38. Gajhede, M., Schuller, D. J., Henriksen, A., Smith, A. T., and Poulos, T. L. (1997) *Nat. Struct. Biol.* **4,** 1032–1038
39. De Ropp, J. S., Mandal, P. K., and La Mar, G. N. (1999) *Biochemistry* **38,** 1077–1086
40. Childs, R. E., and Bardsley, W. G. (1976) *J. Theor. Biol.* **63,** 1–18
41. Poulos, T. L., Freer, S. T., Alden, R. A., Edwards, S. L., Skogland, U., Takio, K., Eriksson, B., Xuong, N. H., Yonetani, T., and Kraut, J. (1980) *J. Biol. Chem.* **255,** 575–580
42. Patterson, W. R., and Poulos, T. L. (1995) *Biochemistry* **34,** 4331–4341
43. Poulos, T. L., Edwards, S. L., Wariishi, H., and Gold, M. H. (1993) *J. Biol. Chem.* **268,** 4429–4440
44. Kunishima, N., Amada, F., Fukuyama, K., Kawamoto, M., Matsunaga, T., and Matsubara, H. (1996) *FEBS Lett.* **378,** 291–294
45. Schuller, D. J., Ban, N., Huystee, R. B., McPherson, A., and Poulos, T. L. (1996) *Structure* **4,** 311–321
46. Henriksen, A., Welinder, K. G., and Gajhede, M. (1998) *J. Biol. Chem.* **273,** 2241–2248
47. Kunishima, N., Fukuyama, K., Matsubara, H., Hatanaka, H., Shibano, Y., and Amachi, T. (1994) *J. Mol. Biol.* **235,** 331–344
48. Choinowski, T., Blodig, W., Winterhalter, K. H., and Piontek, K. (1999) *J. Mol. Biol.* **286,** 809–827
49. Doyle, W. A., Blodig, W., Veitch, N. C., Piontek, K., and Smith, A. T. (1998) *Biochemistry* **37,** 15097–15105
50. Jones, P., and Dunford, H. B. (1977) *J. Theor. Biol.* **69,** 457–470
51. Baek, H. K., and Van Wart, H. E. (1992) *J. Am. Chem. Soc.* **114,** 718–725
52. Smith, A. T., Sanders, S. A., Greschik, H., Thorneley, R. N. F., Burke, J. F., and Bray, R. C. (1992) *Biochem. Soc. Trans.* **20,** 340–345
53. Vitello, L. B., Erman, J. E., Miller, M. A., Wang, J., and Kraut, J. (1993) *Biochemistry* **32,** 9807–9818
54. Fülöp, V., Phizackerley, R. P., Soltis, S. M., Clifton, I. J., Wakatsuki, S., Erman, J., Hajdu, J., and Edwards, S. L. (1994) *Structure* **2,** 201–208
55. Edwards, S. L., Poulos, T. L., and Kraut, J. (1984) *J. Biol. Chem.* **259,** 12984–12988
56. Rodriguez Lopez, J. N., Smith, A. T., and Thorneley, R. N. F. (1996) *J. Biol. Chem.* **271,** 4023–4030
57. Dunford, H. B. (1991) in *Peroxidases in Chemistry and Biology* (Everse, J., and Grisham, M. B., eds) pp. 1–24, CRC Press, Boca Raton
58. Ator, M. A., and Ortiz de Montellano P. R. (1987) *J. Biol. Chem.* **262,** 1542–1551
59. Kraulis, P. J. (1991) *J. Appl. Crystallogr.* **24,** 946–950
60. Bacon, D. J., and Anderson, W. F. (1988) *J. Mol. Graphics* **6,** 219–220
61. Merritt, E. A., and Bacon, D. J. (1997) *Methods Enzymol.* **277,** 505–524
62. Wallace, A. C., Laskowski, R. A., and Thornton, J. M. (1995) *Protein Eng.* **8,** 127–134
63. Smith, A. T., Santama, N., Daceys, S., Edwards, M., Bray, R. C., Thorneley, R. N. F., and Burke, J. F. (1990) *J. Biol. Chem.* **265,** 13335–13343